Ultrafast Electronic Processes in an Insulator: the Be and O Sites in BeO

G. Schiwietz[1*], M. Beye[1], K. Czerski[1,2], A. Föhlisch[1], R. Könnecke[1], M. Roth[1], J. Schlappa[1], F. Staufenbiel[1], E. Suljoti[1], I. Kuusik[3], and P.L. Grande[4]

[1]Institute G-ISRR and former Division SF8, Helmholtz-Zentrum Berlin f. Materialien u. Energie, Hahn-Meitner-Platz 1, 14109 Berlin, Germany

[2]Presently: Inst. Fizyki, Uni. Szczecinski, ul. Wielkopolska 15, 70-451 Szczecin, Poland

[3]Institute of Physics, University of Tartu, Riia 142, 51014 Tartu, Estonia

[4]Uni. Federal do Rio Grande do Sul, Av. Bento Gonçalves 9500, 91501-970 Porto Alegre, RS, Brazil

Abstract

The short-time dynamics of amorphous beryllium oxide (a-BeO) has been investigated for electronic excitation/ionization by fast incident electrons, as well as by Ar^{7+}, Ar^{15+}, Xe^{15+}, and Xe^{31+} ions at velocities of 6% to 10% the speed of light. Site specific Auger-electron spectra induced by fast heavy ions are the central point of this investigation. Electron induced Auger spectra serve as a reference and electron-energy loss (EELS) spectroscopy as well as resonant inelastic x-ray scattering (RIXS) are invoked for quantitative understanding. For the heavy-ion case, we observe strong variations in the corresponding spectral distributions of Be-K and O-K Auger lines. These are related to local changes of the electron density, of the electron temperature and even of the electronic band structure of BeO on a femtosecond time scale after the passage of highly charged heavy ions.

PACS numbers: *79.20.Rf, 71.20.Ps, 31.70.Hq, 32.80.Hd, 61.80.Jh*

Keywords: *Auger-electron emission, ion-track formation, high electronic excitation density, short-time electron dynamics, band-structure variation, wide-gap insulator, melting*

* corresponding author, email: schiwietz(at)helmholtz-berlin.de

1. Introduction

The interaction of fast ions with solids leads to an excitation of a large phase-space volume regarding the electronic degrees of freedom, with only minor nuclear energy-transfers at the same time. Notwithstanding the complexity that arises due to the large variety of ion-solid interaction processes, the primary interaction is extremely well localized in space (typically on an atomic scale) and in time. The time duration of individual energy-transfer processes for fast ions is about 10^{-16} s and less, far below typical electronic or atomic relaxation times. Exactly this separation in time makes the energy-loss of fast ions more or less insensitive to details of the chemical structure and to the Bloch-wave nature of target-electron wave-functions[1]. During recent years, our knowledge on primary energy-transfer processes for intermediate to high velocities has reached a high level of sophistication [2, 3, 4, 5, 6, 7 , 8, 9]. Thus, fast ions are ideal candidates for short-time investigations specifically of electronic relaxation processes in solids.
The corresponding energy dissipation of fast ions in solids is mainly accompanied by various electronic excitations and a large number of electrons may be emitted per primary projectile. Their total number and their energy and angular distributions may be analyzed using electron spectroscopy[10, 11, 12], specifically Auger electron spectroscopy[13, 14], in order to gain information about the early stage of ion-solid interactions. The electronic energy dissipation and relaxation are still subject to intense investigations and effects of the high energy density show up for focused short lasers pulses[15] and for individual slow[16] as well as swift[17] heavy ions.

1.1. Introduction: fast heavy ions in metals

Highly charged ions at specific energies of a few MeV/u (at 10% the speed of light) provide extremely high excitation densities, leading to non-linear effects. At volume energy-densities beyond a certain material-dependent limit, plasmons as well as other (quasi-) particle excitations are overlapping. This leads to a coupling of basic excitations and may have a significant influence on energy-dissipation processes. In principle, a breakdown of usual band-structure-concepts is conceivable, but in most cases indications for a local thermal equilibrium in the electron gas with a Fermi-Dirac distribution at high

electron temperatures and a rapid neutralization of the ion track have been observed [17]. For metals and semi-metals, electron temperatures have been determined from the line-broadening of Auger electrons ejected into the backward hemisphere[17, 18]. For modifications of these materials, either electronic thermal-spike effects[19, 20] or lattice instabilities[21] may play a major role, where hot electrons at electron temperatures up to about 100000 K [22, 23] transfer their kinetic energy or the atomic potential energy to the lattice.

1.2. Introduction: insulator and semiconductor targets

The short-time dynamics of insulators and semiconductor targets displays additional effects in comparison to metals. One of these effects is the evolution of a so-called nuclear-track potential, resulting from an electrostatic cylindrical net charge due to positively charged target-atoms and displaced electrons after primary ionization. Only for very few cases, indications for an ion-track potential have been found. Such a potential may finally lead to materials modifications via the so-called Coulomb explosion[24] of target atoms, but typically the mechanism cannot be traced back from the resulting atomic rearrangements. For shorter times, however, the potential itself shows up in the surface-scattering of molecules[25], or in the penetration of convoy electrons through the surface (polypropylene, PP)[26], or in a strong energy reduction of target Auger electrons (in PP and mylar)[27] in the sub-fs- and fs-time domains. This effect seems to be found mainly for large-band-gap insulators, where electrons may be trapped and holes have low mobility.

For many other materials, such as metals (Al and different metallic glasses) and semi-metals (C and Be), such track potentials have not been found or they are small (for Si). [28] For Si targets we find Auger-energy reductions that maximize for short decay times and for amorphous samples (in comparison to Si(111) crystals with 7x7 reconstruction), reaching 3 eV for very heavy projectile ions,[28] consistent with the spectra measured previously by another group [13]. This relatively small effect (compared to 40 eV for Ne ions on PP) is assigned to a very slow component of the nuclear-track potential with τ_{track} > 30 fs. Very likely, this component is due to self-trapped excitons in the amorphous material, resulting in a slightly reduced electron density in the track. For a crystalline Si

sample, thermally displaced atoms, specifically those close to the surface, might provide meta-stable self-trapping conditions.

In this paper, we concentrate on another short-time effect, namely a possible breakdown of the electronic ground-state band-structure of a specific insulator. Recently, Be Auger-electrons emitted from an ionic BeO surface film due to excitation by fast heavy ions have been investigated for the first time[29]. Here, the Be K-Auger spectra are analyzed in more detail using auxiliary x-ray data for quantitative comparison and K-Auger spectra related to the oxygen site of BeO are presented and analyzed for the first time. As it will be shown, the Auger spectra are neither simply consistent with nuclear-track potentials nor with an electron temperature-broadening or with a combination of both. Similarities and differences of the dynamics for both BeO sites, will be discussed for two K-vacancy configurations in this paper.

2. Experimental method

The experimental UHV setup with the necessary modifications for the BeO experiments has been described in detail previously.[29, 30] Hence, only a short description will be given here. Electron spectra have been taken with a modified electrostatic parallel-plate electron spectrometer involving optimized transmission and energy resolution.[31] The spectrometer was located at a detection angle of 135° with respect to the (normal) incident ion-beam direction inside a doubly magnetically shielded ultra-high vacuum chamber (with typical working pressures close to 10^{-10} mbar dominated by an H_2 contribution).

The channel-plate detector has been shielded against γ-rays from nuclear reactions. As shown previously[29, 32], thin BeO films of about 3 nm thickness[33] have been prepared from atomically clean Be samples either by oxidation using O_2 at elevated temperatures or by implantation of 500 eV oxygen ions. The small thickness of the insulator film prevents macroscopic charging of the surface. Experiments for completely oxidized Be samples have been performed with different heavy ions at specific kinetic energies of a few MeV/nucleon, accelerated by the heavy-ion cyclotron of the ion-beam laboratory ISL Berlin. In this paper, we present data for Ar^{7+} ions at a specific kinetic energy of 3 MeV/nucleon as well as for 1.78 MeV/u Xe^{15+}, both provided directly by the cyclotron.

Charge equilibrated Ar^{15+} ions and Xe^{31+} ions have been extracted behind an additional thin C stripper foil in front of the target (this method provides high charges, actually a distribution of charge states, and suppresses depth dependencies due to charge equilibration near the surface).

Electrons at 2.7 keV have been used as reference projectiles, representative for small perturbations. Using a precision manipulator and a metering orifice for adjusting both beams (electrons as well as ions) at the same point in space, we could make sure that the electron beam (spot size «1 mm) is well focused to the middle of the ion beam spot (Ø ≈ 2 mm) on the target. This adjustment has been tested, e.g., by ion-induced erosion of selenium as well as by amorphization of a silicon crystal. Although the fast projectiles penetrate deep into the target, the emitted electrons investigated in this work stem only from the first few surface layers (Be K-Auger electrons have an inelastic mean-free-path below 1 nm)[34]. In the final ion-beam times presented here, we have used either pure oxygen exposure at about 10^{-6} mbar or alternatively continuous 500-eV O-ion implantation inside the main chamber, in order to prevent any net erosion effect. In both cases, we found time-independent Auger spectra for several hours of ion irradiation as well as for electron irradiation, pointing to dynamically clean and stable surface conditions. We have averaged several raw electron spectra (basic data acquisition time of about 10 minutes) for each of the displayed spectra. No indications have been observed for an exciton-induced surface metallization[35] (this might have been suppressed by the vicinity of the oxide/metal interface or by the global irradiation temperature of ~200 °C) or for complete erosion (needs one to two hours of continuous irradiation when we do not use re-oxidation)[32].

3. Results and Discussion

In the following, results for the two sites of BeO will be presented and discussed independently. Subsequently we will present and discuss results for multiple inner-shell ionization and for the valence-band dynamics of BeO by comparing data for oxygen and beryllium atoms.

3.1. Results and Discussion: The beryllium site of BeO

The Be site of BeO has been investigated recently for incident electrons and incident ions.[29] The electron-induced Be-K Auger-electron spectrum of bulk BeO samples and BeO surface films has been investigated previously also by several other groups[36, 37, 38, 39, 40, 41]. This Auger decay involves an initial K-shell vacancy that becomes filled by an electron resulting from the interaction of two weakly bound electrons. The measured spectra or the corresponding differentiated yields agree well among each other as well as with our measurements for a fully oxidized surface[29]. In this section, we try to provide more details on the Be-K Auger spectra by further analyzing the previously published data and by providing auxiliary x-ray data for a deeper understanding of electronic structure and dynamics of BeO.

Fig. 1 displays Be K-Auger electron spectra for amorphous BeO (a-BeO) around electron energies of 100 eV, where electrons from the ionic O-2s level as well as electrons from the valence band fill a Be-K vacancy. The variation of the spectra is due to a projectile dependence related to fast Ar and Xe ions of different incident charge states and 2.7 keV primary electrons.

As usual, secondary-electron backgrounds have been subtracted by adjusting a fit function to the shape of the Be spectra at energies above 160 eV (below the oxygen Auger structure, the electron yield is dominated by ejected δ electrons) and below 50 eV.[30] Here we allow for two different scaling factors for both energy regions. By doing this, we assume that low-energy shape of the spectrum is given by electron-cascade processes, which should be very similar whether initiated by δ electrons or by Auger electrons. Thus, the resulting Auger spectra after background subtraction will contain the initial Auger structure plus a low-energy wing, representative for electron slowing-down and cascade multiplication. Furthermore, the spectra in Fig. 1 have been separated into single- and double-K-vacancy structures (K^1-XV and K^2-XV), assuming that the low-energy wings of the two structures are related by a linear scaling.[17, 18, 22] Here and in the subsequent text, we use the abbreviation X = L_1 or V (for the L_1 shell and for the valence band V). In fact we found a fit function that fits the peak and part of the low-energy wing simultaneously. The displayed thin solid curve that merges into the K^2-XV peak for 1.78 MeV/u Xe^{31+} ions is an example for such a fit.

The difference of the mean K^2-XV and K^1-XV peak energy is 44 eV, as estimated with

our Hartree-Fock-Slater program[3]. This agrees well with the experimental findings. The high fraction of K^2-XV Auger electrons indicates that multiple ionization is very important, pointing to a strong perturbation of the target electrons. This will be investigated quantitatively at the end this paper. Here we should memorize, however, that the position of the K^2-XV Auger peaks is shifting by about 5 eV at the maximum (by 7 eV at the right shoulder) towards higher energies, when the perturbation is increased from primary electrons to Xe^{31+} ions.

Lets now concentrate on the K^1-XV Auger structure, which consists of several individual peaks, especially for incident electrons (we discuss the evolution of the ion-induced spectra of Fig. 1 at the end of this paper). Using electron energy-loss spectroscopy (EELS) data for our sample and band-structure calculations accounting for the core hole in Be,[42, 43, 44] we could clearly identify most of the peaks.[29] The main peak at 91 eV, is due to K-VV transitions where two electrons of the V_I and V_{II} valence bands (centered around the oxygen site) interact with each other. K-L_1V transitions at 75 eV and K-L_1L_1 transitions at 66 eV (with L_1 related to the O-2s level) have been identified as well. The right-most K^1-XV Auger peak slightly below 102 eV was assigned to a core-hole exciton[45] (excited via shake-up or electron-cascade processes) interacting with a valence-band electron during the decay. The measured peak, however, was not as narrow as expected and it was found 3 eV lower in energy compared to the super-cell band-structure estimate for fixed lattice positions. Making use of auxiliary x-ray data, the solution of this puzzle is presented in what follows.

Fig. 2 displays the spectrum of emitted x-rays from a crystalline BeO sample, taken with the flexRIXS setup and excited by photons from the undulator beamline UE112 of the BESSY II synchrotron in Berlin.[46] For the displayed spectrum, the primary x-ray energy was tuned to the resonance energy of the Be-K core-hole exciton (che) at 119.3 eV. Thus, we investigate resonant inelastic x-ray scattering (RIXS). The structures below the emission energy of 110 eV are due to the decay of BeO spectator states after Be K-vacancy production. They are related to the same states that determine the Auger spectrum in Fig. 1. In fact, use of the line positions in Fig. 2 would have improved our previously published Auger-simulation curve[29] based on band-structure calculations.

The most interesting part of the spectrum in Fig. 2, however, is the x-ray decay of the

core-hole exciton. The sharp line (green curve) at the energy of 119.3 eV is due to elastic resonant scattering and indicates the energy resolution of the whole apparatus. In agreement with a pioneering x-ray investigation of BeO,[47] we find a bi-modal decay structure due to energetic relaxation (involving electron-phonon coupling) of the core-hole exciton. This bi-modal peak structure is indicated also by the two blue arrows in Fig. 1 (denoted che). It explains why the exciton-related Auger structure is found 3 eV lower than expected on the basis of a density-functional calculation without relaxation. The double structure also explains why the measured peak in Fig. 1 is broader than expected beforehand. Furthermore, these x-ray investigations[46, 47] indicate that exciton population and relaxed exciton decay are strongly suppressed by non-resonant and by non-perturbative interactions (interactions of highly charged ions lead to elevated temperatures of the electron systems and of the lattice). Thus, exciton population might have some small influence on the spectra for Ar^{7+} ions in Fig. 1, but probably not significantly on the spectra for ions at higher charge state.

3. 2. Results and Discussion: The oxygen site of BeO

The oxygen site of BeO has not been investigated before with swift heavy ions. However, before we turn to the discussion of ion induced spectra, we should make sure to understand Auger data for incident electron. In this case, only the O-K vacancy will influence the BeO band structure. Fig. 3 displays our O-K Auger data after differentiation (a typical presentation for analytical purposes) together with results by other groups, not corrected for the different spectrometer transmission functions.

This comparison includes a-BeO films from reactive (using an Ar/O_2 gas mixture) rf sputter deposition onto clean metallic Be (measured by Schalch et al.)[41], from slow oxidation of a clean Be surface by residual oxygen contaminations in the UHV system (investigated by Suleman and Pattinson)[38], as well as a poly-crystalline BeO film produced by heating of Be targets to about 600 °C in an oxygen atmosphere (by Soule´ de Bas et al.)[48]. For the data sets by Schalch et al. and by Suleman and Pattinson, energy-scale corrections of +3 eV and +7 eV have been performed, in order to improve the overlap among the different spectra. The statistical fluctuation of our own data is due to averaging of a limited number of electron-reference spectra, taken between the ion runs.

All four electron induced spectra in Fig. 3 are very similar, a signature of a common oxide-target structure. Only the data by Soule´ de Bas et al.[48] seem to show somewhat more pronounced structures, either due the band-structure of the poly-crystalline BeO film or due to a higher resolving power of the electron spectrometer.

Fig. 4 displays two different types of energy spectra taken for our BeO targets. The upper plot shows electron backscattering spectra for 519-eV electrons at an incident angle of 45° with respect to the surface normal. It contains peaks due to elastic backscattering, due to single as well as double collective excitations (bulk-plasmon energy losses). The lower plot shows our original O-K Auger data (without differentiation) as red diamond symbols connected by a smoothed (orange) curve. In this plot, we also provide a semi-quantitative Auger peak analysis, based on the band-structure information, displayed as solid (blue) curve. To a large extend, this simulation is similar to the procedure that we have previously used to assign the peaks of the Be-K Auger spectrum of BeO.[29] A reasonable estimate of the Auger spectrum may be obtained by convoluting the electron populations $dP_X/d\varepsilon$ for each band X with all bands Y, weighted with the *l*-dependent squared Auger matrix elements $M^2_{X,Y}$ (assumed to be energy independent) as well as convoluted with the corresponding energy-loss function $dL/d\varepsilon$ (taken from the upper part of Fig. 4 and broadened by 11 eV) following

$$dN/d\varepsilon = dL/d\varepsilon * \Sigma_{X,Y}\ M^2_{X,Y}\ dP_X/d\varepsilon * dP_Y/d\varepsilon,$$

where the asterisk "*" stands for the convolution operator, similar as in the elaborate Auger treatment in Ref. 49. We have determined $dP_X/d\varepsilon$ from a fit to the partial O density-of-states from our previous band-structure calculation for BeO[29] (note that we have neglected the core-hole effect due to an O-K vacancy) and we have used the approximate relation $M^2_{s,s}=M^2_{p,p}=2\,M^2_{s,p}$ (see Ref. 49). This method neglects surface refraction and final-state hole-hole interaction, but it should be applicable to most cases. Note that the necessary broadening of the spectrum by 11 eV might be an effect of the hole-hole interaction. It can, however, not be explained by the effect of the amorphous BeO target structure (this effective broadening might be 5 eV or less[29]).

It is seen that this model spectrum is not very far from the experimental one. Specifically it contains the full peak structure, namely the two strong peaks at 508 eV and 487 eV and even the small shoulder at about 470 eV. The estimated peak intensities, however, show

significant deviations from the experimental spectrum. This might partially result from an oversimplification of the electron energy-loss treatment or of the scaled matrix elements. However, experience with the Be core-hole suggests that relaxation of the electron density in the surrounding of the K ionized oxygen site might be important for the band structure.

As one may see, the peak assignment in Fig. 4 is not straight forward. Only the Auger peak at the highest energy (508 eV) is clearly due to K-VV transitions where two electrons of the V_I and V_{II} valence bands are active in the decay. The other two peaks are combinations of plasmon shoulders and Auger transitions involving the O-L_1 state. We are confident, however, that we understand the gross features of the Auger spectrum for incident electrons. After the above discussion of the Auger spectrum due to fast primary electrons, related to perturbative interactions with the target electrons, we will focus in the following on strong perturbations as they are produced by highly charged ions at a similar particle velocity (at specific kinetic energies of a few MeV/u).

Fig. 5 displays a series of O K-Auger electron spectra for a-BeO around electron energies of 500 eV, where electrons from the ionic O-2s level and mainly electrons from the valence bands fill an O-K vacancy. Secondary-electron backgrounds have been subtracted and the resulting spectra have been separated into single- and double-K-vacancy contributions (O-K^1-XV and O-K^2-XV and the corresponding dashed curves used for extrapolation), as described for the data in Fig. 1. The black solid curve shows the data for primary electrons at 2.7 keV, already discussed in the proceeding two figures. The variation of the spectra in Fig. 5 is due to the projectile dependence related to the strong electrostatic interaction of fast Ar and Xe ions for different incident charge states. From these spectra one may extract that the position of the O K^1-XV Auger peaks is shifting by about 8 eV at the maximum (by 10 eV at the high-energy wing) towards higher energies, when the perturbation is increased from primary electrons to Xe^{31+} ions. Furthermore, it is seen that the ion-induced spectra involve a double-peak structure with a fixed peak-to-peak distance of 20 eV, consistent with the two uppermost peaks for incident electrons. Thus, the whole spectral structure seems to be shifting to higher energies as function of the perturbation.

Furthermore, the shape of the energy-loss shoulder at energies below the Auger lines is

clearly different from the incident-electron case. The extreme variation of the spectral structure for the Be atom seems to hide this effect (see Fig. 1), but it is in agreement with practically all ion- and electron-induced spectra investigated so far.[17] It is not unlikely that this smearing out and background-enhancement is due to enhanced energy-loss rates (reduced mean free paths) of Auger electron leaving the hot electron gas around the ion track. A similar Auger-electron absorption in a hot electron gas was observed in the angular distribution of Auger electrons from ion tracks.[50]

The K^2-XV peaks for 1.78 MeV/u Xe^{31+} ions are very strong. They are centered 20 to 35 eV above the K^1-XV peaks. A more accurate statement on this energy shift is not possible since the spectral shapes are extraordinary broad (much broader than any of the previously observed target Auger lines for fast incident ions) and a peak maximum for the K^2-XV structure is not visible. Theoretically we expect a shift of about 55 eV between single and double oxygen K-vacancy, estimated with our Hartree-Fock-Slater program (assuming full initial-state screening)[3]. The experimentally determined shift of the maximum energy of the high-energy wings of the O-K^1-XV and O-K^2-XV structures is 66 eV (somewhat higher than our theoretical estimate).

3. 3. Results and Discussion: Double K-vacancies in BeO

Finally, we discuss the most important features of the spectra in Figs. 1 and 5, trying to deduce a consistent interpretation of the dynamics in a-BeO after penetration of fast highly charged ions. In order to get an inside on the strength of the interaction between the heavy ions and our BeO films, we concentrate first on multiple inner-shell ionization of the Be and O sites. Previously, we have performed such investigations for the carbon K-shell and for the silicon L-shells.[17] In this paper, we present such data for the first time for heavy ions interacting with a compound target.

Fig. 6 displays experimentally determined cross section ratios for the double K-shell ionization divided by the total ionization (single plus double). For O and Be atoms we proceed from the spectra in Figs. 1 and 5 in an equal way. For the single- and for the double-K-vacancy contributions (after background treatment and separation), we integrate the spectra from an energy of about 50 eV (just above the cascade-electron peak) to the high-energy end of the corresponding Auger structure. The resulting yields

$Y(K^2)$ and $Y(K^1)$ have to be corrected for the analyzer resolution (proportional to the electron energy E) and for the electron escape length (roughly proportional to $E^{1.8}$). The single ionization yield is also affected by a small additive correction due to δ-electron induced K vacancies[51] (we assume 3% for O and 10% for the Be case). After applying these three corrections (analyzer, depth of origin, δ-electron cascades) we arrive at the corrected yields $Y'(K^2)$ and $Y'(K^1)$. Finally, the corrected-yield ratio $Y'(K^2)/Y'(K^1)$ corresponds already to the wanted cross section fraction $\sigma(K^2)/ [\sigma(K^1)+ \sigma(K^2)]$, since practically each Auger electron from double ionization is followed afterwards by a K^1-XV transition (here we neglect the fraction of x-ray transitions of about 1%).
The symbols in Fig. 6 show that the fractional double ionization cross section is strongly increasing with the modulus of the incident projectile charge state or equivalently with the perturbation strength. The ratio for Be-K increases from value of about 0.4% for incident electrons to 22% for the heaviest ions. For O-K vacancies there exists only a faint indication of an electron induced double ionization (probably due to shake-off processes) and a meaningful ratio can't be deduced from the present data. Heavy ions, however, lead to a very strong double ionization fraction, up to 64% for 1.78 MeV/u Xe^{31+} ions. Even more information may be extracted from the shape of the fit curves. These fit curves resemble roughly the behavior of the quantum mechanical first-order Magnus approximation[52, 53] or full coupled-channel calculations[3]. Within perturbation theory, ionization probabilities for each independent electron are proportional to the squared projectile charge q^2. Hence, double ionization is proportional to q^4, single ionization to q^2 and thus, the ratio should follow q^2 for small values of q. At high charge state non-perturbative theories predict (mainly) a saturation of the cross section ratio beyond a certain projectile charge. This saturation regime seems to be reached for Be at $q>10$ and for O at $q>20$. These saturation regimes are related to ionization probabilities of 100% per electron (for zero impact parameter) at the center of the ion track. Thus, for the strongest perturbation (1.78 MeV/u Xe^{31+} ions), we expect ionization of **all** electrons (K- and L-shells for both species as well as the local valence-band population) at the center of the ion tracks.

3. 4. Results and Discussion: Spectral variations of the ion-induced Auger lines

Let us now try to derive a common picture through a more detailed analysis of Figs. 1 and 5. First, we should be aware that the investigation of Auger spectra of Be and O for single and double ionization is related to snapshots of the time evolution of the electronic system. For single Be-K ionization we estimate an extremely long Auger decay time of $\tau(\text{Be-K}^1) = 300$ fs, by scaling the known decay time of metallic Be with the partial density of states of our band-structure calculation.[29] The ionic character of BeO leads to an increase of $\tau(\text{Be-K}^1)$ on one hand and on the other hand it leads to a reduction of the corresponding value for single ionization of O-K, namely $\tau(\text{O-K}^1) = 3$ fs. For double-K ionization there are two possible K vacancies open for the decay, which doubles the Auger rate corresponding to $\tau(\text{Be-K}^1) = 150$ fs and $\tau(\text{O-K}^1) = 1.5$ fs. For the strongest perturbations we expect that the Auger clock is stopped for a short time after the complete local ionization, since there are nearly no electrons close to the K vacancies and Auger decay is impossible. Later on the electrons return, but restoration of the ionic character takes an additional time. Thus, Be and O might separately be neutral, giving rise to hot-state decay times of $2\tau^*(\text{Be-K}^2) = \tau^*(\text{Be-K}^1) = 16$ fs and $2\tau^*(\text{O-K}^2) = \tau^*(\text{O-K}^1) = 5$ fs, as expected in the extreme for the Be metal and free O atoms. Thus, for the heavy ions it seems hardly possible to derive an accurate decay time, specifically for Be-K vacancies. Nevertheless, there is a clear time order, where $\tau^*(\text{O-K}^2) < \tau^*(\text{O-K}^1) < \tau^*(\text{Be-K}^2) < \tau^*(\text{Be-K}^1)$. Below, we will discuss the different spectra along this time line.

a) The O K^2-XV Auger structures do not show any visible peak maximum and they are they extremely broad, not comparable to any of our previously investigated Auger spectra. The mean energy of this structure seems to be lower than our theoretical energy estimate. The high-energy edge is somewhat higher (by 10 to 20 eV) than expected on the basis of this perturbative estimate. This could be an indication for a high electron temperature (leading to the high edge energies) and for a neutralization of a strong track potential during the Auger-decay time. Considering the fast Auger decay within about 2 fs and the strong perturbation due to double K-ionization, a superposition of both effects is conceivable. But the broad spectrum does not allow a quantitative evaluation of such effects.

b) The shapes of the O K^1-XV Auger peaks due to incident ions are related to the structure measured for incident electrons. They contain typical effects of a high electron temperature (broadened high-energy edge and enhanced energy-loss shoulder below the peak maximum). However, we find a positive shift of the O K^1-XV Auger maximum by about 8 eV towards higher energies for the heaviest ions. Note that a possible influence of an ion-track potential would lead to an energy reduction and not an energy increase.[17] A possible explanation for this positive shift will be given below.

c) The Be K^2-XV Auger structures for incident ions show a broadening of the high-energy edge that increases with the perturbation. Compared to the small Be K^2-XV peak for incident electrons (not visible in this scale), the ion induced spectra as a whole shift to higher energies (by about 5 eV) with increasing perturbation. Thus, the Be K^2-XV spectra show features similar to the O K^1-XV Auger peaks, with a slightly weaker projectile dependence. The positive Auger-energy shift seems to be too strong to be exclusively due to an electronic population-density shift, directly related to the high electron temperatures (this would require temperatures above about 500,000 K, inconsistent with the high-energy wings of the Auger structures). A more likely explanation for the observed shift is the closing of the energy gap of BeO, known for high lattice temperatures[54] and also expected for non-equilibrium electronic potentials. If we assume a nearly symmetrical closing of the gap[54], the valence-band edge would shift to higher energies by up to 5 eV per electron (for the metallic state). An upper estimate for the equilibrated high-temperature limit of the resulting Auger-peak shift (involving 2 valence-band electrons and a completely closed gap) is 10 eV, and thus, only slightly above the measured values of 5 to 8 eV.

d) Let us now concentrate on the Be K^1-XV Auger structure, which consists of several individual peaks. This richness of peaks allows discussing the variation from electron-induced to ion-induced spectra in greater detail. According to our estimates, this Auger structure corresponds to the smallest transition rate and thus, to the longest K-decay time. One may observe from Fig. 1 that all peaks below 98 eV are increasingly strong suppressed as a function of the perturbation (for more

highly charged ions). At a kinetic energy of 102 eV (about 0.5 eV above the core-hole exciton peak for incident electrons), a single sharp peak seems to be growing with increasing perturbation. Finally, for Xe^{31+} ions, however, only a single asymmetric high-energy peak or cut-off is visible with a nearly smooth and relatively flat low-energy background. It is noted that the Be core-hole exciton is of minor importance for the heavy-ion induced spectra, as follows from the discussion below and from the remarks concerning Fig. 2.

The shape variation shown in Fig. 1 is in contrast to all previous Auger investigations (for metals, semi-metals, metallic glasses, semi-conductors, and even polymers) [10, 12, 13, 17, 22, 23, 27, 30]. Specifically, the electron- and ion-induced spectra in Fig. 1 are inconsistent with each other on the basis of the product of the Fermi-Dirac distribution $f(\varepsilon,T_e)$ and the electronic density of states $D(\varepsilon)$, since a strong suppression of low-energetic peaks (for high electron temperatures T_e) would populate not only a single peak (with a continuous electron energy-loss background) but produce a very long high-energy tail for single as well as for double ionization. Thus, the spectra in Fig. 1 show a clear **breakdown of the ground-state band-structure**, where also $D(\varepsilon)$ varies significantly with the electron temperature T_e.

It is also noted that the average energy of the main Be K^1-XV Auger structure (evaluated at energies above 81 eV) shifts from 91.9 eV to 98.7 eV. This positive shift of 6.8 eV is consistent with the energy shifts found for O K^1-XV and Be K^2-XV and it seems to be related to a partial or even complete closing of the energy gap. Additional information may be extracted from the asymmetric shape of the Auger spectrum found for Xe^{31+} ions. Such a structure-less background below a high-energy cut-off was visible even more clearly for fast Au^{41+} ions on partly oxidized BeO samples, published previously.[29] The shape and position of this peak were shown to agree well with Be K^1-XV spectra for the same ion beam on a pure Be metal surface (without any energy gap). We take this agreement as a strong indication for a **metallic character of BeO after excitation by heavy ions.** In other words, we expect a complete closing of the energy gap of BeO.

4. Conclusion

We have investigated the electronic excitation/ionization of amorphous beryllium oxide by fast incident electrons, as well as by Ar^{7+}, Ar^{15+}, Xe^{15+}, and Xe^{31+} ions at similar velocities of 6% to 10% the speed of light. We have analyzed the Be-K Auger spectra in more detail than previously (considering also results from resonant inelastic x-ray scattering RIXS) and we have presented an EELS spectrum for a typical O-K Auger energy as well as ion-induced O-K Auger spectra for the first time. Comparing incident electrons with incident heavy ions, we observe a strong variation in the corresponding spectral distributions of Be-K and O-K Auger lines. This is related to changes in the local electronic environment and even to a breakdown or instability of the electronic ground-state band-structure of BeO at higher electron temperatures. The investigation of single- as well as double-ionization for both lattice sites, yields snapshots of the short-time dynamics on a femtosecond time scale after the passage of charged particles. Materials modifications may be excluded from the interpretation, since the electron induced spectra taken in between the ion runs guarantee steady-state conditions, related to our methods of continuous surface oxidation during the experiments.

In summary, the different Auger spectra and side information lead us to the following consistent interpretation of the data. From the ratio of double to single K-ionization we infer an extremely strong perturbation of all electronic states, involving even complete ionization of the atomic electrons on the central path of a heavy ion inside BeO. For times below about 2 fs (the O K^2-XV Auger structures) we find indications for a high electron temperature at the high-energy edge. Furthermore, there seems to be a very strong ion-track potential (the smearing out of the whole Auger structure towards lower energies) that is not visible at later time steps. Thus, by that first time step the ion track is not fully neutralized. The widths of the high-energy wing for subsequent time steps (the Auger structures O K^1-XV as well as Be K^2-XV and Be K^1-XV) point to electron temperatures between 60 000 and 120 000 K for heavy ions.

These three spectra also involve a shift of the mean peak position by about 5 to 8 eV towards higher energies, related to a switching of the band structure from an insulating ionic to a metallic character (corresponding to a complete closing of the energy-band gap). In fact, at kinetic electron energies above 80 eV, the Be K^1-XV structure may be

decomposed for each projectile into an insulator spectrum (taken for incident electrons) and a structure-less asymmetric peak representing the metallic state. This switching might be a direct electronic band-structure effect due to the modified screening at high electron temperatures,[29] but the estimated long decay time for Be K^1-XV transitions (somewhere between 20 and 200 fs) points to a stabilization of this non-equilibrium state. A possible solution of this puzzle might be an ultra-fast cold melting of the lattice[21, 55] (also known as spontaneous lattice relaxation[56]), which might keep the energy-gap closed even on a picosecond timescale. The answer to this question, however, calls for further research on the subject.

Acknowledgements

We are indebted to the ISL-cyclotron crew of the former Hahn-Meitner-institute for providing stable and intense ion beams and to the BESSY II-synchrotron crew for providing excellent x-ray operation conditions. Last but not least we should mention the help by K. Kunnus and S. Schreck regarding the x-ray detection system and many helpful physics discussions with S. Klaumünzer. Further, we acknowledge funding by the Alexander-von-Humboldt foundation, by CNPq and by CAPES.

Figures

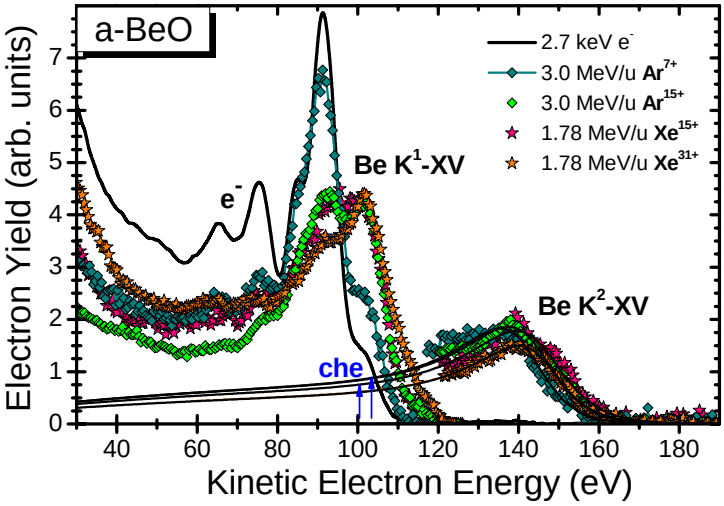

Fig. 1: (colour online) Projectile dependence of the Be K-Auger spectrum for a-BeO due to fast Ar and Xe ions of different incident charge states (averaged over many raw spectra) and 2.7 keV electrons. Spectra have been separated into single- and double-K-vacancy peaks (K^1-XV and K^2-XV) after subtraction of secondary-electron backgrounds.

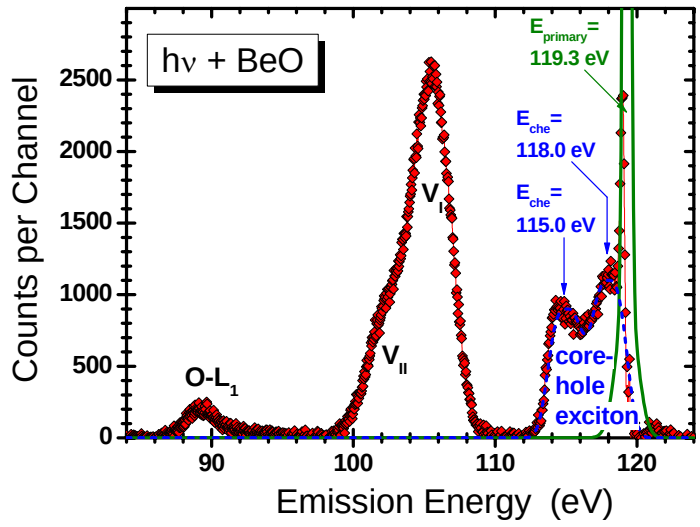

Fig. 2: (colour online) Resonant inelastic x-ray scattering (RIXS): Emitted x-ray spectrum obtained for the primary x-ray energy tuned to the resonance energy (119.3 eV) of the Be-K core-hole exciton (che). After subtraction of a background due to diffuse scattering inside the x-ray spectrometer, an elastic-scattering peak (fitted green solid curve) has been subtracted from the spectrum resulting in the (red) diamond symbols.

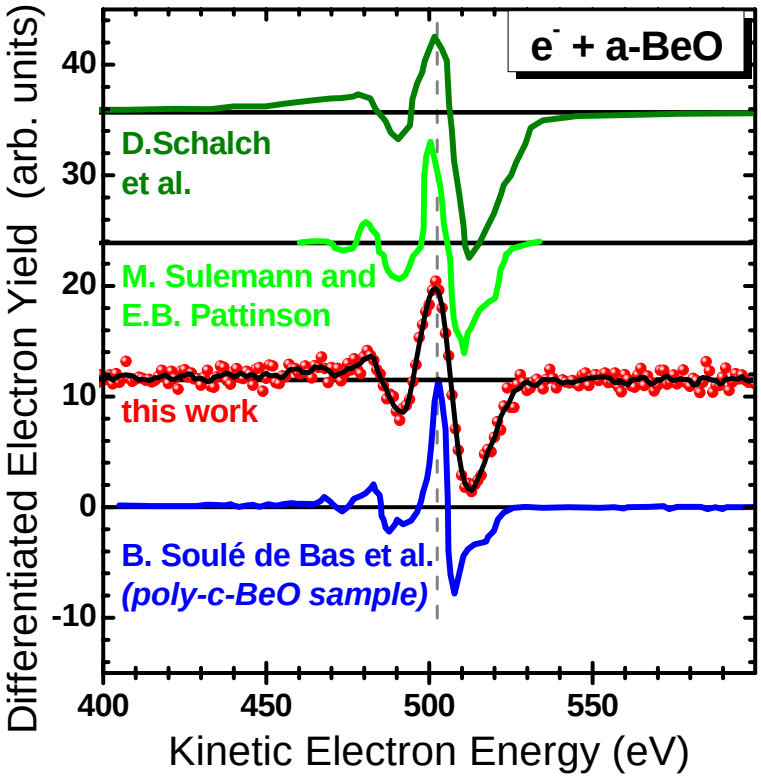

Fig. 3: (colour online) Differentiated O-KXV electron spectra. The (red) circles and smoothed (black) curve were obtained in this work (averaged over a few spectra induced by 2.7 keV electrons during the heavy-ion beam times). Other curves are taken from the literature and correspond also to a-BeO[38, 41] as well as to poly-crystalline BeO (poly-c-BeO)[48].

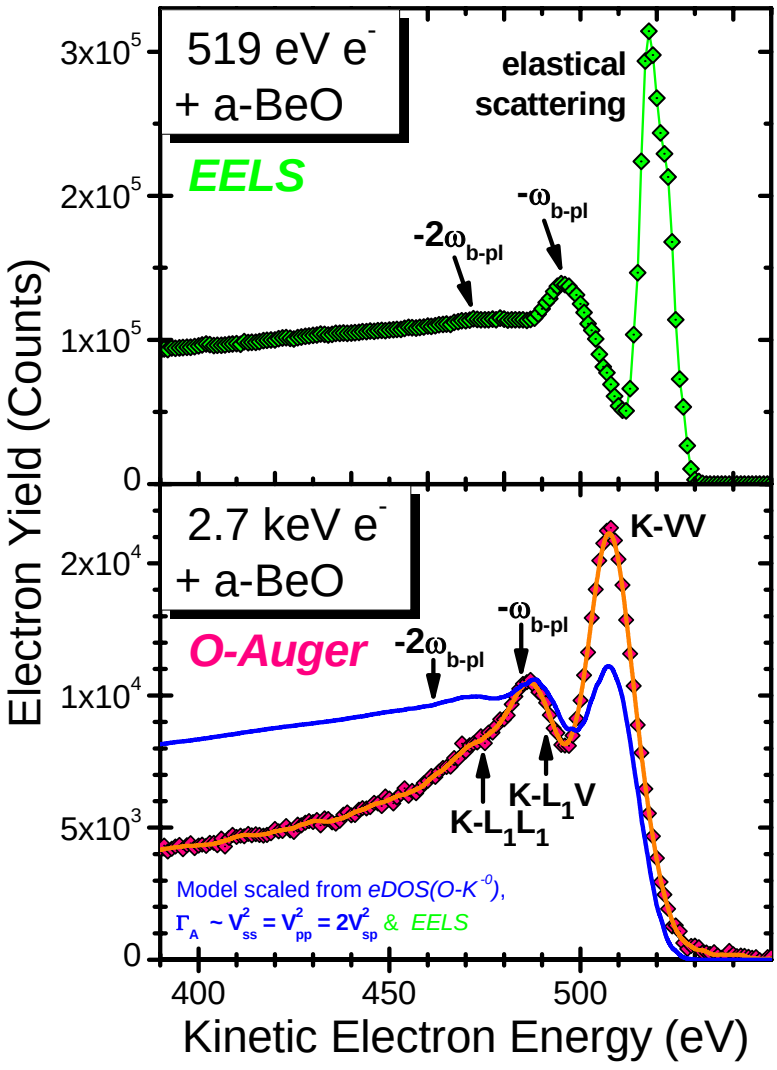

Fig. 4: (colour online) Electron energy-loss spectrum (*EELS* in the upper plot) for 519 eV primary electrons and O KXV-Auger electron-spectrum (*O-Auger* in the lower plot) due to primary 2.7 keV electrons (after subtraction of the δ-electron background), both for the a-BeO target. The solid blue curve shows a simulation of the Auger spectrum as described in the text.

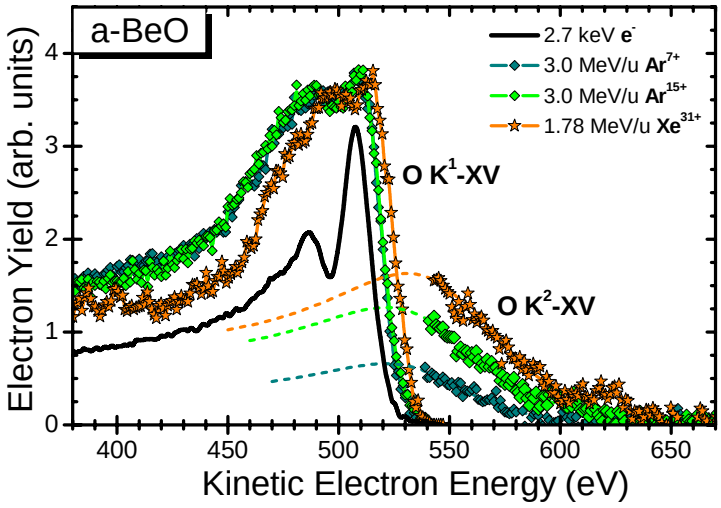

Fig. 5: (colour online) Projectile dependence of the O K-Auger electron spectrum for a-BeO due to fast ions of different incident charge states (averaged over several raw spectra) and 2.7 keV electrons. Spectra have been separated into single- and double-K-vacancy peaks (K^1-XV and K^2-XV) after subtraction of secondary-electron backgrounds.

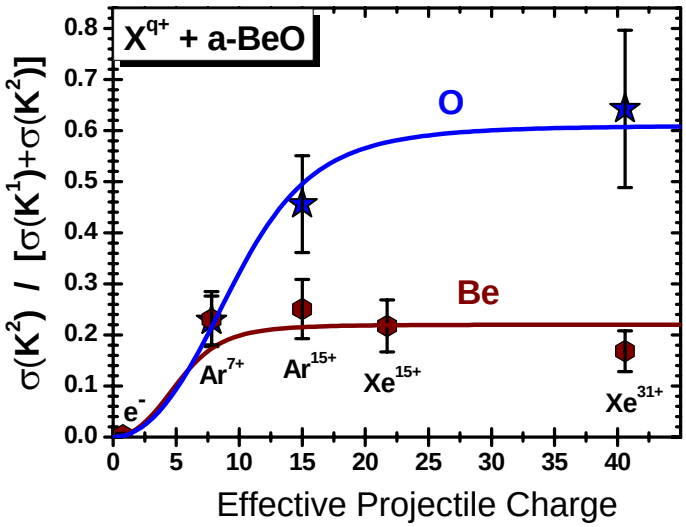

Fig. 6: (colour online) Fractional experimental double-K-vacancy cross sections, determined from the ratio of Auger yields (K^2-XV and K^1-XV) as function of an effective projectile charge for incident electrons and heavy ions. The (blue) asterisk symbols correspond to K vacancies at the O sites and the (wine) coloured hexagons are related to Be-K ionization. The evaluation procedure (including corrections) is described in the text and the solid curves are to guide the eye.

References

[1] G. Schiwietz and P.L. Grande, "Electronic Stopping Based on Atomic and Solid-State Wavefunctions", Radiation Effects and Defects in Solids **130/131**, 137-156 (1994).

[2] P. Sigmund and A. Schinner, Nucl. Instr. and Meth. **B195**, 64 (2002); P. Sigmund, Kongelige Danske Vidensk. Selskab: Matematisk-Fysiske Meddel. **Vol. 52**, 557-593 (book article ed. by P. Sigmund, 2006).

[3] P.L. Grande and G. Schiwietz; in "Advances in Quantum Chemistry", **Vol. 45**, pp.7-46 (book article ed. by J. Sabin, 2004, Elsevier Inc.).

[4] C.C. Montanari, J.E. Miraglia, and N.R. Arista, Phys. Rev. **A66**, 042902 (2002).

[5] A. Arnau, M. Penalba, P.M. Echenique, F. Flores and R.H. Ritchie, Phys.Rev.Lett. **65**, 1024 (1990).

[6] A.F. Lifschitz and N.R. Arista, Phys. Rev. **A69**, 012902 (2004).

[7] P.D. Fainstein, G.H. Olivera and R.D. Rivarola, Nucl. Instr. Meth. **B107**, 19-26 (1996).

[8] G. Schiwietz and P.L. Grande, "Introducing Electron Capture in the UCA Energy-loss Theory at Low Velocities", Phys.Rev. **A84**, 052703 (2011).

[9] A. Hentz, G.S. Parkinson, P.D. Quinn, M.A. Muñoz-Márquez, D.P. Woodruff, P.L. Grande, G. Schiwietz, P. Bailey, T.C.Q. Noakes; "Direct observation and theory of trajectory-dependent electronic energy losses in medium-energy ion scattering", Phys.Rev.Lett. **102**, 096103 (2009).

[10] D.Hasselkamp, "Particle Induced Electron Emission II", Springer tracts of modern physics, **Vol. 123**, (Springer, Berlin, 1991) and references therein.

[11] H. Rothard, Scanning Microscopy **9** , 1 (1995).

[12] A. Koyama, H. Ishikawa, K. Maeda, Y. Sasa, O. Benka, and M. Uda, Nucl. Instr. Meth. **B48**, 608 (1990).

[13] W. Schmidt, P. Müller, V. Brückner, F. Löffler, G. Saemann-Ischenko, and W. Schubert, Phys. Rev. **A24**, 2420 (1981).

[14] G. Schiwietz, G. Xiao, E. Luderer, and P.L. Grande; "Auger Electrons from Ion Tracks", Nucl. Instr. Meth. **B164-165**, 353-364 (2000).

[15] R. Stoian et al., Phys.Rev.Lett. **88**, 097603 (2002).

[16] A. Arnau et al., Surface Science Reports **27**, Issues 4-6, 113 (1997).

[17] G. Schiwietz, M. Roth, K. Czerski, F. Staufenbiel, and P.L. Grande, "Femtosecond Dynamics: Snapshots of the Early Ion-Track Evolution", Nucl. Instr. Meth. **B226**, 683–704 (2004); and references therein.

[18] G. Schiwietz, G. Xiao, P.L. Grande, E. Luderer, R. Pazirandeh, U. Stettner; "An Experimental Determination of Electron Temperatures in the Center of Nuclear Tracks in Amorphous Carbon", Nucl. Instr. Meth. **B146** , 131-136 (1998).

[19] Z.G. Wang, C. Dufour, E. Paumier and M. Toulemonde, J.Phys.: Cond. Matter **6**, 6733 (1994).

[20] K. Sokolowski-Tinten et al., Phys. Rev. Lett. **81/1**, 224 (1998).

[21] P. B. Hillyard et al. Phys. Rev. Lett. **98**, 125501 (2007).

[22] F.Staufenbiel et al., Nucl. Instr. Meth. **B230**, 426 (2005); G. Schiwietz et al., Europhys. Lett. **47**, 384 (1999).

[23] M. Caron, H. Rothard, M. Beuve, B. Gervais; Physica Scipta **T92**, 281 (2001).

[24] R.L. Fleischer, P.B. Price, and R.M. Walker, 'Nuclear Tracks in Solids' (University of California Press, Berkely California, 1975).

[25] M. Sakata, K. Nakajima, M. Suzuki, K. Kimura, "Grazing scattering of 1–2 MeV HeH+ ions from KCl(0 0 1): Effect of surface track potential", Nucl. Instr. Meth. **B269**, 795–798 (2011).

[26] G. Xiao, G. Schiwietz, P.L. Grande, N. Stolterfoht, A. Schmoldt, M. Grether, R. Köhrbrück, A. Spieler, U. Stettner; "Indications of Nuclear-Track-Guided Electrons Induced by Fast Heavy Ions in Insulators" Phys. Rev. Lett. **79/10**, 1821-1824 (1997) and references therein.

[27] G. Schiwietz, P.L. Grande, B. Skogvall, J.P. Biersack, R. Köhrbrück, K. Sommer, A. Schmoldt, P. Goppelt, I. Kádár, S. Ricz, U. Stettner; "Influence of Nuclear Track Potentials in Insulators on the Emission of Target Auger Electrons", Phys. Rev. Lett. **69**, 628-631 (1992).

[28] G. Schiwietz, K. Czerski, R. Hellhammer, M. Roth, F. Staufenbiel, R.C. Fadanelli, and P.L. Grande; "Search for short-time phase effects in the electronic damage evolution - a case study with silicon", Nucl. Instr. Meth. **B266**, 1287–1293 (2008).

[29]G. Schiwietz, K. Czerski, M. Roth, P.L. Grande, V. Koteski, and F. Staufenbiel; "Evidence for an Ultrafast Breakdown of the BeO Band Structure Due to Swift Argon and Xenon Ions", Phys.Rev.Lett. **105**, 187603 (2010). ibid; "Ultrafast Band-Structure Variations Induced by Fast Au Ions in BeO", Nucl. Instr. Meth.**B269**, 959-963 (2011).

[30] G. Schiwietz, K. Czerski, M. Roth, F. Staufenbiel, E. Luderer, P. L Grande; "Si-Auger electrons from the center of nuclear track", Nucl. Instr. Meth. **B193**, 705-712 (2002); the 2pVV surface plasmon assignment in that paper is false, as follows from a more detailed analysis [see ref. 28].

[31] G. Schiwietz, M. Roth, and F. Staufenbiel, German patent 10 2008 058 144, "Elektrostatischer Energieanalysator für geladene Teilchen, Spektrometer und Monochromator mit einem solchen Analysator".

[32] K. Czerski, G. Schiwietz, M. Roth, F. Staufenbiel, P.L. Grande and S.R. Bhattacharyya; "Non-equilibrium emission of secondary ions from BeO films sputtered by swift gold ions", Nucl. Instr. Meth. **B225**, 72-77 (2004).

[33] Estimated using the SRIM-2008 code, see also "The Stopping and Range of Ions in Solids", by J.F. Ziegler, J.P. Biersack and U. Littmark, (Pergamon Press, New York, 1985/2009).

[34] NIST Standard Ref. **Database 100** for the Simulation of Electron Spectra for Surface Analysis (SESSA 1.1); see also W. Smekal, W. S. M. Werner, and C. J. Powell, Surf. Interface Anal. **37**, 1059 (2005).

[35] T. Neidhart et al., Phys.Rev.Lett. **74**, 5280 (1995).

[36] D.M. Zehner, N. Barbulesco and L.H. Jenkins, Surface Science **34**, 385 (1973).

[37] D.E. Fowler and J.M. Blakely, J. Vac. Sci. Technol. **20**(4), 930 (1982).

[38] M. Suleman and E.B. Pattinson, J. Phys. F: Metal Phys. **3**, 497 (1973).

[39] M. Euler, A. Scharmann, Physica Status Solidi (a) **34/1**, 297 (1976).

[40] H.H. Madden, Surface Science **126/1-3**, 80 (1983).

[41] D. Schalch, A. Scharmann and A. Weiß, Thin Solid Films **124**, 351 (1985).

[42] Super-cell calculations based on density-functional theory[44] have been performed using the WIEN97 code[43] for the EDOS of an Be^{+} ion inside the atomically frozen ground-state BeO (Wurtzite) structure[29].

[43] P. Blaha, K. Schwarz and J. Luitz, WIEN97, Karlheinz Schwarz, Techn. Univ. Wien, Austria (1999) ISBN 3-9501031-0-4.

[44] P. Hohenberg and W. Kohn, Phys. Rev. **136**, B864 (1964); W. Kohn and L.J. Sham, Phys. Rev. **140**, A1133 (1965).

[45] J.A. Soininen et al., J. Phys.: Cond. Matter **13,** 8039 (2001).

[46] M. Beye, A. Föhlisch, R. Könnecke, I. Kuusik, G. Schiwietz , J. Schlappa, and E. Suljoti, (2012, in preparation).

[47] A. Kikas, T. Käämbre, K. Kooser, I. Kuusik, V. Kisand, E. Nommiste, M. Kirm, E. Feldbach, V. Ivanov, V. Pustovarov, and I. Martinson, J. Phys. Condens. Matter **22**, 375505 (2010); I. Kuusik, T. Käämbre, K. Kooser, V. Pustovarov, V. Ivanov, E. Kukk, and A. Kikas, Journal of Electron Spectroscopy and Related Phenomena **184**, 366 (2011).

[48] B. Soule´ de Bas, H.E. Dorsett, and M.J. Ford, Journal of Physics and Chemistry of Solids **64,** 495 (2003).

[49] J.E. Houston, J.W. Rogers, R.R. Rye, F.L. Hutson, D.E. Ramaker, Phys. Rev. B **34**, 1215 (1986).

[50] G. Schiwietz, M. Roth, K. Czerski, F. Staufenbiel, and P.L. Grande; "Indications for enhanced Auger-electron absorption in a hot electron gas", Phys.Rev.Lett. **99**, 197602 (2007).

[51] G. Schiwietz, D. Schneider, J.P. Biersack, N. Stolterfoht, D. Fink, A. Mattis, B. Skogvall, H. Altevogt, V. Montemayor, U. Stettner; "Cascade-Induced Asymmetry in Auger-Electron Emission Following Fast Ion-Solid Interactions", Phys. Rev. Lett. **61**, 2677-2680 (1988).

[52] H. Ryufuku and T. Watanabe, Phys. Rev. **A18**, 2005 (1978); Phys. Rev. **A19**, 1538 (1979).

[53] U. Wille, J . Phys. B: At. Mol. Phys. **16**, L275 (1983).

[54] M. Beye, F. Hennies, M. Deppe, E. Suljoti, M. Nagasono, W. Wurth and A. Föhlisch; "Measurement of the predicted asymmetric closing behaviour of the band gap of silicon using x-ray absorption and emission spectroscopy", New Journal of Physics **12**, 043011 (2010).

[55] P.L. Silvestrelli, M. Parrinello, J. Appl. Phys. **83**, 2478 (1998).

[56] P. Stampfli, K.H. Bennemann, Phys. Rev. **B49**, 7299 (1994); P. Stampfli, Nucl. Instr. and Meth. **B107**, 138 (1996).